

Coordination Chemistry in the Solid: Evidence for Coordination Modes within Hybrid Materials Different from those in Solution

Robert J. P. Corriu,^{*[a]} Frank Embert,^[a] Yannick Guari,^[a] Catherine Reyé,^[a] and Roger Guilard^[b]

Abstract: Two routes of incorporation of europium(III) salts into cyclam-containing hybrid materials have been explored, to elucidate the coordination mode of Eu^{III} in cyclam-containing hybrid materials in a study of the arrangement of cyclam moieties during the sol–gel process. They were 1) complexation of europium salts by N-tetra-substituted 1,4,8,11-tetraazacyclotetradecane (cyclam) derivatives bearing four hydrolysable Si(OEt)₃ groups, followed by hydrolysis and polycondensation of

these complexes; and 2) hydrolysis and polycondensation of N-tetra-substituted silylated cyclam derivatives, then incorporation of europium salts directly into the hybrid materials. The coordination mode of europium salts within solids is not the same as in solution. In solution, the complexation of Eu^{III} with cyclam is

Keywords: amorphous materials • coordination modes • cyclams • europium • sol-gel processes

not possible; it requires cyclam derivatives containing N-chelating substituents such as amido groups in an appropriate geometry. In contrast, the incorporation of Eu^{III} into hybrid materials is always possible, whatever the nature of the arms of the cyclam moieties. Thus, Eu^{III} uptake is one Eu^{III}/two macrocycles with cyclam moieties containing *N*-alkyl substituents. This constitutes the first example of 4N+4N lanthanide coordination.

Introduction

Nanostructured organic–inorganic hybrid materials^[1, 2] are obtained by hydrolytic polycondensation of molecular precursors bearing more than one hydrolysable Si(OR)₃ group. They constitute a new class of materials obtained under mild conditions and including organic units covalently linked to the inorganic silica matrix (Scheme 1).

One of the essential characteristics of such systems is their short-range autoorganisation ability during the sol–gel process, which has been demonstrated^[2] by their chemical properties^[3] and by small-angle X-ray scattering (SAXS).^[4] Besides, evidence of long-range organisation in the solid has been provided by birefringence experiments in the case of rigid organic moieties.^[5] These results were then extended to more flexible models.^[6]

We have also recently described^[7] the incorporation of CuCl₂ within nanostructured cyclam-containing hybrid mate-

rials obtained by hydrolytic polycondensation of the molecular precursor **1** (Scheme 2).

This route of incorporation of Cu^{II} into cyclam-containing hybrid materials allows the complexation of one Cu^{II}/cyclam moiety. Interestingly, it gives rise to copper–copper interactions, evidenced by ESR spectroscopy.^[7] Such interactions have been observed from ESR measurements in solution of dinuclear Cu^{II} complexes specifically designed for this purpose, in which two cyclam rings are in a face-to-face conformation (Figure 1).^[8] Furthermore, these materials possess an oxygen bonding capacity,^[9] which has never been observed for Cu^{II} complexes in solution.

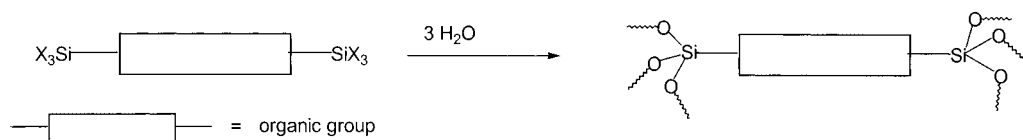
The existence of copper–copper interactions obtained by the direct incorporation of CuCl₂ into cyclam-containing hybrid materials involves an arrangement of cyclam moieties during the sol–gel process in such a way that they are in close proximity to each other. Such an organisation would probably be due to the hydrophobic character of the tetra-*N*-propyl cyclam moieties, opposed to the hydrophilic part around the silicon atom [RSi(OR)_{*x*}(OH)_{3-*x*}] formed during the sol–gel process.

To obtain further evidence concerning the arrangement of cyclam moieties during the sol–gel process, we studied the incorporation of Eu^{III} into cyclam-containing hybrid materials for three reasons.

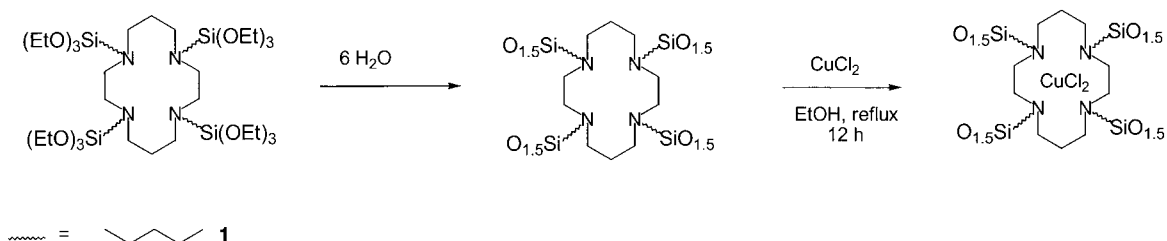
1) The coordination mode of lanthanide ions is very different from that of Cu^{II}; lanthanide complexes exhibit coordina-

[a] Prof. R. J. P. Corriu, Dr. F. Embert, Dr. Y. Guari, Prof. C. Reyé
Université de Montpellier II
34095 Montpellier, Cedex 5 (France)
Fax: (+33)467143852
E-mail: corriu@crit.univ-montp2.fr

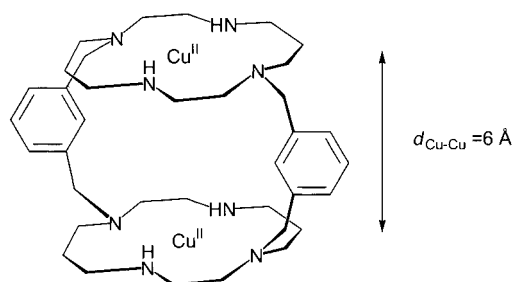
[b] Prof. R. Guilard
UMR 5633, Université de Bourgogne
6 boulevard Gabriel, 2100 Dijon (France)



Scheme 1.



Scheme 2.

Figure 1. Face-to-face conformation of Cu^{II} cyclam complexes.

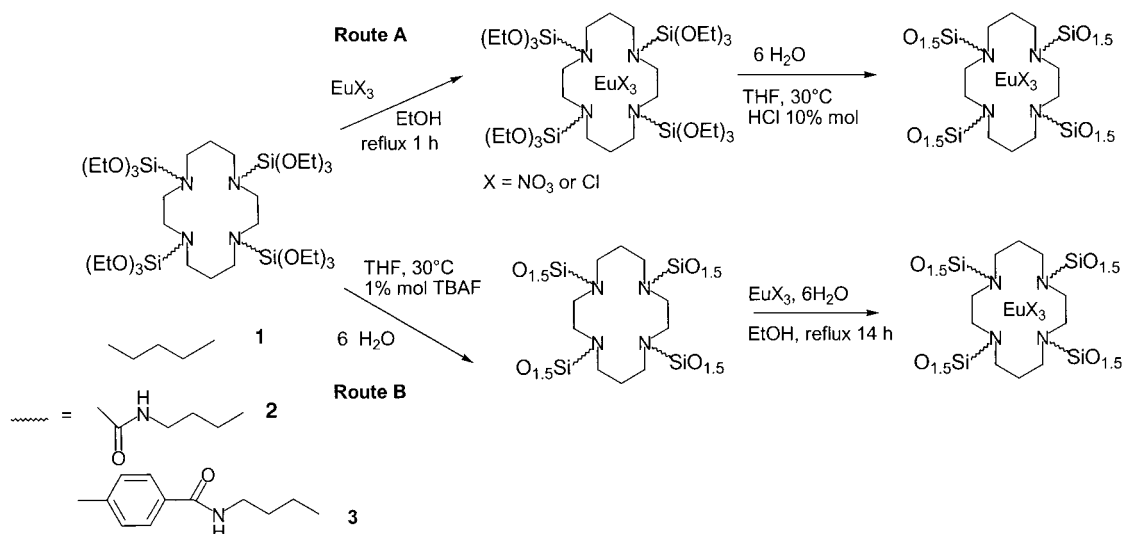
tion numbers ranging from six to twelve, with eight and nine being the most common.^[10]

- 2) In solution, the complexation of Cu^{II} by cyclam moieties occurs whatever the nature of the N substituents of the cyclam. In contrast, the 1,4,8,11-tetraazacyclotetradecane (cyclam) does not complex lanthanide ions in solution. The complexation of lanthanide ions requires N-substituted cyclam derivatives with four pendant arms containing chelating groups, because of their high coordination number.

- 3) Eu^{III} is a luminescent centre displaying multiple emissions whose relative intensities and line splitting patterns are very sensitive to the bonding environment around the metal ion.^[10, 11]

Herein, two routes of incorporation of Eu^{III} salts into cyclam-containing hybrid materials are described (Scheme 3). We have prepared three silylated N-tetra-substituted cyclam derivatives (Scheme 3): **1** contains four pendant arms without chelating groups and consequently unable to complex lanthanide ions in solution; **2** contains four pendant arms with chelating groups^[12] allowing the complexation of lanthanide ions in solution; **3** appears as an intermediate model in which the pendant arms bear chelating groups, but the rigidity of these arms does not allow the complexation of lanthanide ions in solution.

We show that the coordination mode of Eu^{III} in cyclam-containing hybrid materials is very different from that in solution. Indeed, whereas the molecular precursor **2** is the only one able to complex Eu^{III} in solution, thus allowing the incorporation of the salt by route A in Scheme 3 (gelation of the isolated Eu^{III} complex), the incorporation of the europium salts into the solid by route B in Scheme 3 is always possible,

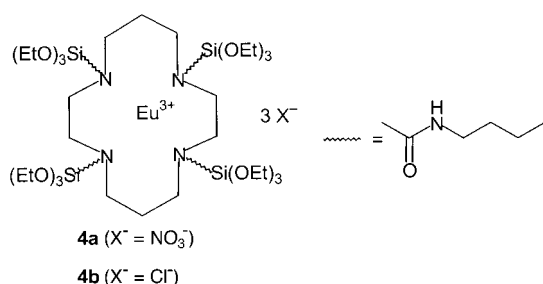


Scheme 3.

whatever the nature of the pendant arms (gelation of **1**, **2** or **3**, then incorporation of Eu^{III} into the hybrid materials). Furthermore, we show that the amount of the europium salts incorporated by route B depends on the nature of the *N*-substituents of the cyclam moieties.

Results and Discussion

Cyclam derivative **1** was prepared as previously described.^[13] Treatment of the cyclam with 2-bromo-*N*-triethoxysilylpropylacetamide (4 equiv) afforded **2** in 97% yield. The reaction of the cyclam with *p*-chloromethyl-*N*-triethoxysilylpropylbenzamide (4 equiv) gave **3** in 76% yield. Treatment of a boiling solution of anhydrous europium salt (nitrate or chloride) in ethanol with **2** (4 equiv) in boiling ethanol afforded the corresponding europium salt complexes **4a** and **4b** in high



yield; these were identified as 1:1 complexes. All attempts to isolate crystals suitable for X-ray analysis failed. FTIR experiments gave evidence that the reaction was complete. Indeed, both the C=O stretching vibrations of the free ligand were shifted to lower frequencies (30 to 37 cm⁻¹ for the upper band I and 21 to 27 cm⁻¹ for the other one), indicating that all the amido groups are involved in the formation of **4a** and **4b** (Table 1). We checked that, as expected, no reaction took place when **1** or **3** was treated with a boiling ethanol solution of the europium salt.

Table 1. C=O stretching vibrations ($\nu(\text{C}=\text{O})$ [cm⁻¹]) for **2** and the corresponding europium complexes.

2	4a	4b
1684.0	1648.5	1648.5
1646.1	1621.8	1621.8

Preparation and characterisation of hybrid materials obtained from complexes **4a** and **4b** (Scheme 3, route A):

The hydrolytic polycondensation of complexes **4a** and **4b** was performed at 30 °C in a THF solution containing H₂O (6 equiv), under acidic conditions (10 mol % HCl). Gelation of **4a** and **4b** was also carried out under nucleophilic conditions (1 or 10 mol % tetrabutylammonium fluoride (TBAF) as catalyst). However we have observed that the gelation

times are always shorter under acidic conditions than under nucleophilic conditions, probably owing to the strong tendency of Ln^{III} complexes to coordinate small ions such as F⁻.^[14, 15] The gels were allowed to age for five days at the gelation temperature. They were then powdered, washed with ethanol, acetone and diethyl ether, and dried under vacuum at 120 °C for 14 h.

We will consider only the solids prepared under acidic conditions. The dried gels were named **SZ**, where **S** indicates solid (xerogel) and **Z** is the number characterising the precursor (**4a** or **4b**). Physical data for these solids are reported in the Experimental Section. The BET surface areas were very low (< 10 m² g⁻¹). Their elemental analyses indicate that the complexation survives the hydrolytic polycondensation as the experimental ratio Eu/N is close to the expected one (see the Experimental Section).

Preparation and characterisation of hybrid materials obtained from **1**, **2** and **3** (Scheme 3):

The hydrolytic polycondensation of **1**, **2** and **3** was performed at 30 °C in THF solution containing H₂O (6 equiv) and in the presence of TBAF (1 mol %) as catalyst. Translucent colourless monoliths were obtained. The gels underwent the work-up described above. ¹H NMR analysis of the filtrates revealed no traces of precursor.

The solid-state ²⁹Si NMR spectra of the xerogels displayed a set of resonance signals lying between $\delta = -45.2$ and -77 ppm assigned to T¹ [C-Si(OR)₂OSi], T² [C-Si(OR)(OSi)₂], and T³ [C-Si(OSi)₃] substructures (Table 2). The absence of a resonance signal corresponding to Q substructures^[16] (in the $\delta = -100$ ppm region) indicated that no cleavage of Si-C bonds occurred during the sol-gel process. The degree of condensation τ of the hybrid materials was evaluated by deconvolution of the individual T resonance signals.^[17-19] The degree of condensation of **S1** is fairly high, whereas the xerogels **S2** and **S3** are very condensed (Table 2). Powder X-ray diffraction data for the xerogels showed that they are amorphous. The BET surface areas S_{BET} determined by adsorption-desorption of N₂ were very low (< 10 m² g⁻¹) for **S2** and **S3**. The BET surface area of **S1** was over 300 m² g⁻¹. The complete elemental analysis of these materials (Table 2) confirms the conservation of the cyclam moieties within them.

Direct incorporation of Eu(NO₃)₃ · 6H₂O and of EuCl₃ · 6H₂O into the xerogels **SZ** (Z = 1–3) (Scheme 3, route B):

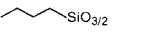
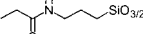
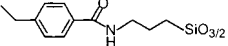
We checked that the incorporation of Eu^{III} did not take place in the absence of cyclam moieties inside the solids: a silica prepared from TEOS was treated with a solution of Eu(NO₃)₃ · 6H₂O in ethanol heated under reflux for 14 h. After filtration of the solid and washing with ethanol, elemental analyses of the silica revealed no trace of europium.

Table 2. ²⁹Si CP MAS NMR data and elemental analysis of xerogels **S1**–**S3**.

	²⁹ Si CP MAS NMR data [%]			τ [%]	Elemental analysis	
	T ¹	T ²	T ³		calcd formula	exp. formula
S1	-45.2(3)	-59.1(50)	-66.3(47)	81	C ₂₂ H ₄₄ N ₄ O ₆ Si ₄	C _{23.4} H _{48.5} N _{3.9} O _{9.3} Si _{4.0}
S2	(0)	-57.6(24)	-66.2(76)	92	C ₃₀ H ₅₆ N ₈ O ₁₀ Si ₄	C _{31.1} H _{62.0} N _{8.0} O _{12.9} Si _{4.1}
S3	(0)	-57.4(10)	-65.9(90)	97	C ₅₄ H ₇₂ N ₈ O ₁₀ Si ₄	C _{56.2} H _{77.7} N _{8.0} O _{13.3} Si _{4.1}

The xerogels **SZ** ($Z = 1–3$) were treated with an excess of $\text{Eu}(\text{NO}_3)_3 \cdot 6\text{H}_2\text{O}$ or $\text{EuCl}_3 \cdot 6\text{H}_2\text{O}$ (2 equiv Eu^{3+} /cyclam moiety within the solids) in ethanol solution. The mixture was heated under reflux for 14 h. The resulting solids were washed copiously with ethanol and diethyl ether to eliminate the uncomplexed salt, until no traces of nitrate were detected by FTIR spectroscopy in the concentrated filtrate. They were named **SZ[EuX₃]**, where **S** and **Z** are as defined above and EuX_3 represents the salt. Table 3 summarises elemental analyses of xerogels dried under vacuum (120 °C, 13 h, 0.1 mmHg). Surprisingly, the direct incorporation of europium salt appeared possible by route B in all cases, even that of **S1** prepared from the precursor **1**, which does not contain chelating arms. However, the Eu^{III} uptake per macrocycle is highly dependent on the nature of the N substituents of the macrocycle. It is even greater than one Eu^{III} /macrocycle for **S3**.

Table 3. Eu^{III} uptake into xerogels **S1**–**S3**.

Xerogel	N substituent of the macrocycle	Eu^{III} uptake [equiv Eu^{III} /macrocycle] ^[a]
S1[EuCl₃]		0.65
S1[Eu(NO₃)₃]		0.51
S2[EuCl₃]		0.74
S2[Eu(NO₃)₃]		0.80
S3[Eu(NO₃)₃]		1.12

[a] Determined from elemental analysis.

Preparation of co-gels from 1 and 2 and confirmation of the proportion of Eu^{III} incorporated into S1 and S2 (Scheme 4): Elemental analyses of xerogels **S1[Eu(NO₃)₃]** and **S2[Eu(NO₃)₃]** have indicated the presence of approximately one Eu^{III} /cyclam for **S2[Eu(NO₃)₃]** and one Eu^{III} /two cyclams for **S1[Eu(NO₃)₃]**. This last result suggests the proximity of cyclam moieties within the hybrid material, allowing the complexation of one equivalent of Eu^{3+} between two tetraazamacrocycles. This is in agreement with the previous study of the incorporation of Cu^{II} into the same material.^[7]

For further proof of this result, we have studied the incorporation of $\text{Eu}(\text{NO}_3)_3$ into materials obtained by co-hydrolysis and polycondensation of **1** or **2** with tetraethoxysilane (y equiv; $y = 5, 10, 15, 40$) to scatter the cyclam moieties into silica. Scattering of the cyclam moieties within the materials prepared from **2** should not alter the Eu^{III} /

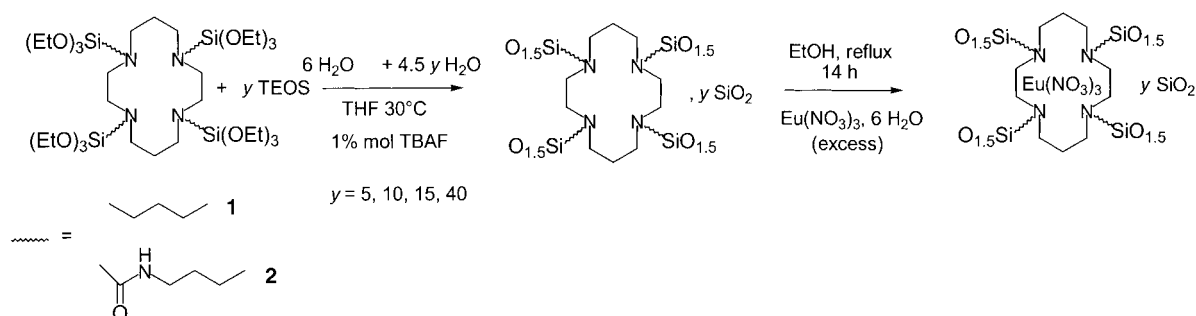
cyclam ratio if it is of one Eu^{III} /cyclam moiety. In contrast, the Eu^{III} uptake within the materials prepared from **1** should decrease as y increases, the distance between the cyclam moieties becoming greater and greater.

The co-hydrolysis and polycondensation of the precursor **1** or **2** with TEOS (y equiv) was performed in the presence of TBAF (1 mol%) as catalyst, at 30 °C in THF solution containing the stoichiometric amount of water (Scheme 4). Dried gels obtained after the usual work-up (see the Experimental Section) were named **S_yZ**, where **S** indicates solid (xerogel), the index y specifies the number of equivalents of TEOS and **Z** is the number characterising the precursor (**1** or **2**).

Both types of co-gels **S_y1** and **S_y2** ($y = 5, 10, 15, 40$) were treated with an excess of an ethanol solution of $\text{Eu}(\text{NO}_3)_3 \cdot 6\text{H}_2\text{O}$ (2 equiv Eu^{III} /cyclam moiety) heated under reflux for 14 h. The resulting solids **S_y1[Eu(NO₃)₃]** and **S_y2[Eu(NO₃)₃]** were washed copiously with ethanol at room temperature to eliminate the non-complexed salt until no traces of $\text{Eu}(\text{NO}_3)_3$ were detected in the filtrate. The extent of the complexation reaction was determined by elemental analysis of the materials after they had been dried under vacuum (120 °C, 14 h, 0.1 mmHg) (Table 4). The results show clearly that the Eu^{III} /cyclam ratio does not change with the composition of the co-gels **S_y2**, which is in agreement with an uptake of about one Eu^{III} /cyclam moiety; however, it decreases notably for **S_y1** when $y = 40$. This result is in agreement with the coordination of one Eu^{III} between two cyclam moieties.

FTIR and thermal analysis of xerogels: The FTIR spectra of xerogels **S4a** and **S4b** (route A) revealed that the C=O stretching vibrations (bands I) within the solids are very close to those of the starting complex, indicating that there was no decomplexation during the sol–gel process (compare Table 1 and Table 5).

The FTIR spectra of xerogels **S2[Eu(NO₃)₃]** and **S2[EuCl₃]** (route B) display two bands attributed to the stretching vibration of C=O groups and very close to those observed for the xerogels **S4a** and **S4b** (route A) but they are different from that observed for **S2** (solid without Eu^{III}) (Table 5). This suggests strongly that the incorporation of europium salts according to route B involves most of the C=O groups. The FTIR spectrum of **S3[Eu(NO₃)₃]** exhibits two C=O stretching bands (1644 and 1620 cm^{-1}). As the FTIR spectrum of **S3** displays a band at 1643 cm^{-1} , it can be concluded that in this case not all the C=O groups are involved in the complexation



Scheme 4.

Table 4. Eu^{III} uptake into co-gels **S₁** and **S₂**.

sample	Calc. stoichiometry	Exp. stoichiometry	Equiv. of Eu ^{III} /cyclam moiety ^[a]
S1 [Eu(NO ₃) ₃]	C ₂₂ H ₄₄ Eu _{0.3} N _{5.5} O _{10.5} Si ₄	C _{23.8} H _{54.4} Eu _{0.51} N _{5.7} O _{18.3} Si _{4.0}	0.51
S₅1 [Eu(NO ₃) ₃]	Eu _{0.5} N _{5.5} Si ₉	Eu _{0.54} N _{5.1} Si _{9.0}	0.54
S₁₀1 [Eu(NO ₃) ₃]	Eu _{0.5} N _{5.5} Si ₁₄	Eu _{0.47} N _{5.0} Si _{14.0}	0.47
S₁₅1 [Eu(NO ₃) ₃]	Eu _{0.5} N _{5.5} Si ₁₉	Eu _{0.44} N _{4.5} Si _{19.0}	0.44
S₄₀1 [Eu(NO ₃) ₃]	Eu _{0.5} N _{5.5} Si ₄₄	Eu _{0.23} N _{4.6} Si _{44.0}	0.23
S2 [Eu(NO ₃) ₃]	C ₃₀ H ₅₆ Eu ₁ N ₁₁ O ₁₉ Si ₄	C _{35.1} H _{58.7} Eu _{0.80} N _{8.8} O _{19.5} Si _{4.0}	0.80
S₅2 [Eu(NO ₃) ₃]	Eu ₁ N ₁₁ Si ₉	Eu _{0.86} N _{9.7} Si _{9.0}	0.86
S₁₀2 [Eu(NO ₃) ₃]	Eu ₁ N ₁₁ Si ₁₄	Eu _{0.82} N _{9.4} Si _{14.0}	0.82
S₁₅2 [Eu(NO ₃) ₃]	Eu ₁ N ₁₁ Si ₁₉	Eu _{0.75} N _{9.4} Si _{19.0}	0.75
S₄₀2 [Eu(NO ₃) ₃]	Eu ₁ N ₁₁ Si ₄₄	Eu _{0.80} N _{10.0} Si _{44.0}	0.80

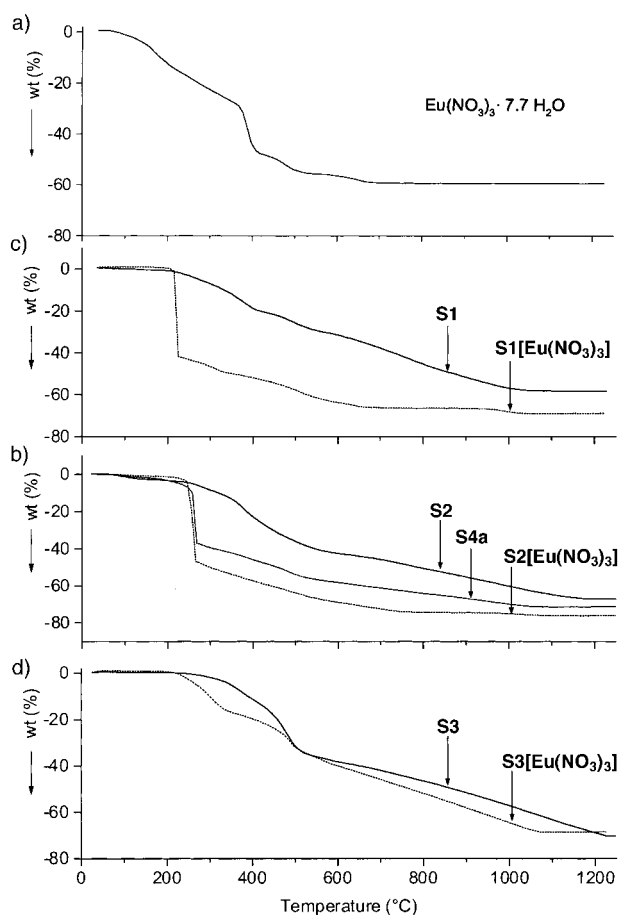
[a] Determined from elemental analysis.

Table 5. Stretching vibrations [cm⁻¹] for C=O groups in various materials containing Eu^{III} salts.

S2	S4a	S2 [Eu(NO ₃) ₃]	S4b	S2 [EuCl ₃]
1665	1649	1648	1648	1653
	1622	1624	1622	1627

of Eu^{III} ions, the band at 1644 cm⁻¹ being attributed to the free C=O groups.

Thermogravimetric analyses (TGA) of xerogels **SZ** (**Z** = 1–3) and of xerogels containing europium nitrate incorporated by each route were performed under air, from room temperature to 1200 °C. The TGA patterns for **S4a**, **S2**[Eu(NO₃)₃] (Figure 2c) and **S1**[Eu(NO₃)₃] (Figure 2b) are

Figure 2. TGA curves (air, 10 °C min⁻¹) for a) Eu(NO₃)₃ · 7.7 H₂O; b) **S1**, **S1**[Eu(NO₃)₃]; c) **S2**, **S4a**, **S2**[Eu(NO₃)₃]; d) **S3**, **S3**[Eu(NO₃)₃].

very similar: after the removal of water, there is a sharp weight loss attributed to the nitrate groups, occurring within a very narrow temperature range, followed by a progressive weight loss assigned to the organic groups up to 1200 °C. Interestingly, the TGA patterns of Eu(NO₃)₃ · 7.7 H₂O (Figure 2a) as well as that of **S3**[Eu(NO₃)₃] (Figure 2d) are very different. The loss of the nitrate groups occurs within a wide temperature range for both of them. For **S3**[Eu(NO₃)₃], there is a progressive and concomitant loss of the nitrate groups and the organic groups (Figure 2d): onset of decomposition occurs at about 200 °C with complete oxidation by about 1200 °C. In this last case, the TGA pattern is very similar to those of materials **S1**, **S2** and **S3** that do not contain europium nitrate (Figure 2b–d), for which the loss of the organic groups occurs from about 200 to 1200 °C.

As the three nitrate groups are bidentate to Eu³⁺ ions for Eu(NO₃)₃ · 7.7 H₂O,^[19] we have concluded that the nitrate groups are also bidentate to Eu^{III} within **S3**[Eu(NO₃)₃], whereas they are not within **S4a**, **S2**[Eu(NO₃)₃] and **S1**[Eu(NO₃)₃]. That should explain the rapid loss of the nitrate groups in these last cases.

Thus, when the ligand **2** with amido groups as pendant arms is used, the nitrate groups are not involved in the complexation of Eu^{III}, whatever the route of incorporation of Eu^{III}. They are not involved in the complexation of Eu^{III} even with the ligand **1**, although the propyl “arms” cannot take part in the complexation. In contrast, taking into account the TGA curve, the nitrate groups should be bidentate on Eu^{III} within the xerogels **S3**[Eu(NO₃)₃] whereas the ligand **3** bears pendant arms with chelating groups.

Photoluminescence of materials at 2 K: Luminescence spectra of Eu^{III} are known to exhibit an extraordinary sensitivity to the ligand environment.^[10] Therefore we took advantage of the luminescence behaviour of our amorphous materials to gain more information on the environment around the metal centres.

The luminescence of the xerogels was measured at 2 K under laser excitation at 325 nm. The emission lines of the xerogel in the Eu^{III} emission spectrum for **S4a** (Figure 3) were assigned to the transitions from the ⁵D₀ level to the ⁷F_{*j*} (*j* = 0–4) levels (Figure 3). The ⁵D₀–⁷F₀ transition is of particular interest as neither the ⁵D₀ nor the ⁷F₀ state can be split by the crystal field.^[10] The number of components observed for this transition is then related to the number of chemically distinct

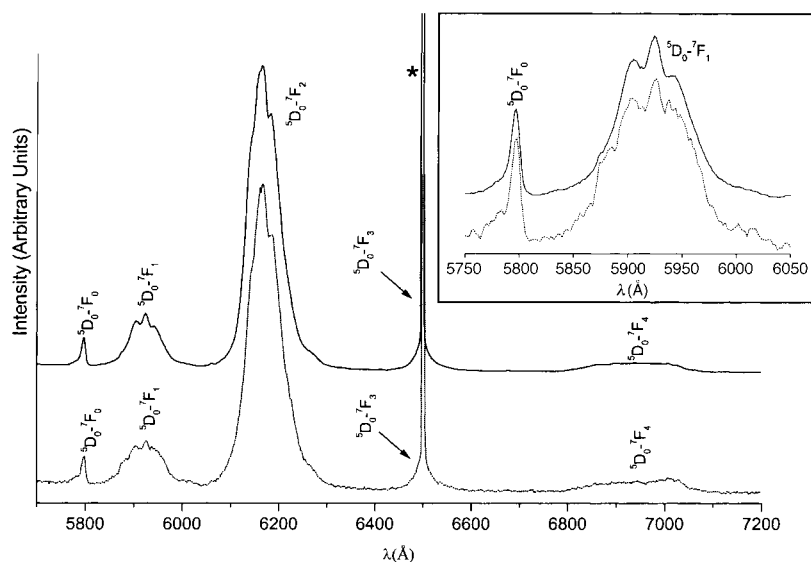


Figure 3. Emission spectra of xerogels **S4a** (top, —) and **S2[Eu(NO₃)₃]** (bottom, ----) recorded under laser excitation at 325 nm at 2 K. * Corresponds to second-order scattered laser beam.

environments of the Eu^{III} ion and the transition has been used as a probe of sample homogeneity. Only one line is observed for the material **S4a** prepared by hydrolysis and polycondensation of isolated complex **4a** by route A (Figure 3). Thus, in this material, the bonding environment of Eu^{III} is unique, confirming that the complexation of Eu^{III} survives the sol–gel process without any change.

The emission spectrum of **S2[Eu(NO₃)₃]** (Figure 3) prepared by route B differs from that of **S4a** in several respects.

- 1) There is a shoulder for the ⁵D₀–⁷F₀ transition in addition to the main line, in contrast with the unique line for **S4a**.
- 2) The line for the ⁵D₀–⁷F₁ transition is split into three components for **S4a**, which indicates only one type of Eu³⁺ bonding site, whereas for **S2[Eu(NO₃)₃]** the hyperfine structure of the ⁵D₀–⁷F₁ transition is much more complicated.

These observations show that the incorporation of Eu^{III} into **S2** (route B), in which the cyclam moieties have adopted certain conformations, gives rise to a Eu^{III}-doped material that is not perfectly homogeneous.

In the emission spectra of both **S1[Eu(NO₃)₃]** and **S3[Eu(NO₃)₃]** (Figure 4), a broad shoulder is observed in addition to the main ⁵D₀–⁷F₀ line, as well as splitting into more than the three components obtained for the ⁵D₀–⁷F₁ transition. This indicates that different environments exist around Eu^{III} within these materials.

Thus, the luminescence study of these materials shows the

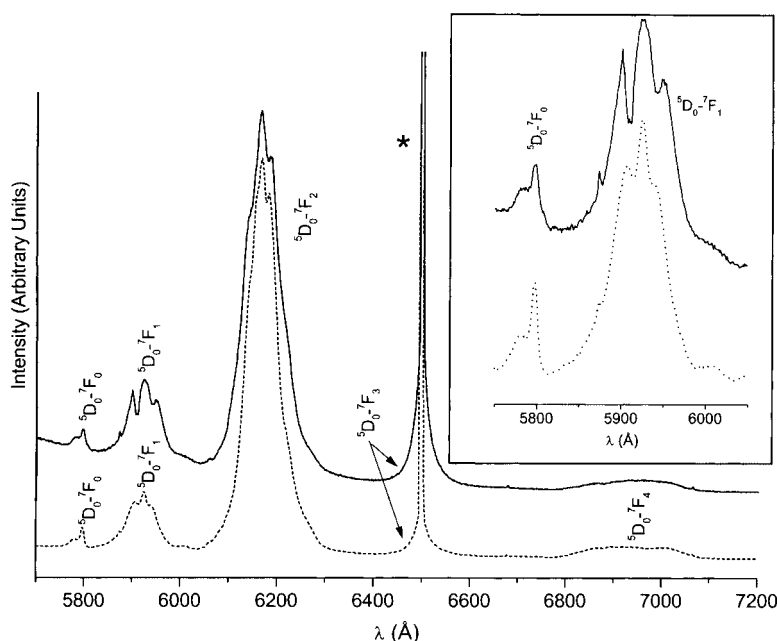


Figure 4. Emission spectra of xerogels **S1[Eu(NO₃)₃]** (top, —) and **S3[Eu(NO₃)₃]** (bottom, ----) recorded under laser excitation at 325 nm at 2 K. * Corresponds to second-order scattered laser beam.

hypersensitive character of the ⁵D₀–⁷F₀ and ⁵D₀–⁷F₁ transitions to the ligand environment.

Coordination mode of Eu^{III} within the cyclam-containing hybrid materials: In spite of the amorphous character of our solids, from the physical data described in this paper we propose a coordination mode for Eu^{III} within the different materials.

Among the three cyclam derivatives that we have prepared, **2**, which contains amido groups, is the only one able to complex Eu^{III} in solution. In contrast, the direct incorporation of Eu^{III} within the cyclam-containing hybrid materials is always possible, even if the N substituents of the cyclam moieties are not chelating (precursor **1**).

This great difference between the coordination mode of Eu^{III} in solution and in the solid state results from the entropy of the solid being lower than that of the solution, which allows the formation in the solid state of complexes that are unstable in solution.

Coordination mode of Eu^{III} within S4a, S4b and S2[Eu(NO₃)₃]: The main inferences from the analytical data of these materials are that:

- 1) FTIR spectra of xerogels have revealed that most of the C=O groups are coordinated to Eu^{III}.
- 2) Thermal analyses of these three materials have shown that the nitrate groups are not bidentate to Eu^{III}.

3) The luminescence spectrum of **S4a** (route A) has revealed that the bonding environment around Eu^{III} is unique within these materials, whereas within $\text{S2}[\text{Eu}(\text{NO}_3)_3]$ the first coordination sphere of Eu^{III} is weakly disturbed by a crystal field of a different nature.

Therefore we propose a coordination mode of one Eu^{3+} /cyclam moiety for **S4a** and **S4b** (route A). The Eu^{III} would probably be eight-coordinate and located between the four nitrogen atoms of the macrocycle and the four oxygen atoms of the amido groups (Figure 5).

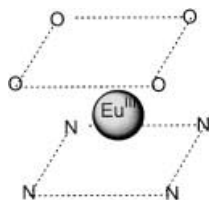
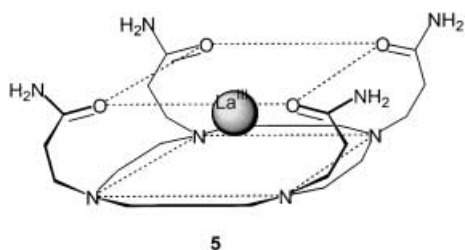


Figure 5. Proposed coordination mode within **S4a** and **S4b**.

Though the ring size is of importance for the coordination mode of lanthanide cations as well as that of metallic cations,^[21–23] the coordination mode that we propose would be rather similar to that observed in the crystal structure of the lanthanum complex **5**^[24] of the cyclen derivative. (To the best of our knowledge, there is no example of the crystal structure of a lanthanide complex of a cyclam derivative bearing neutral chelating ligands.)



In **5**, obtained in anhydrous conditions, the lanthanum(III) ion is eight-coordinate and is encapsulated by the four nitrogen atoms of the macrocycle and the four oxygen atoms of the amido groups. The nitrogen and oxygen atoms involved in the primary coordination sphere lie in two planes that are almost parallel.

We also propose a coordination mode of one Eu^{III} /cyclam moiety within $\text{S2}[\text{Eu}(\text{NO}_3)_3]$, although the Eu^{III} load is 0.8 equiv/cyclam moiety for $\text{Eu}(\text{NO}_3)_3$ and 0.74 for EuCl_3 . This coordination mode is strongly suggested by the elemental analysis results of co-gels **Sy2**. In this case, it is not the organisation of cyclam moieties occurring during the sol–gel process which controls the complexation of Eu^{III} , as each cyclam moiety can complex Eu^{III} independently of the other units.

The incorporation of Eu^{III} into **S2** may be less than one Eu^{III} /cyclam moiety because the hydrolysis and polycondensation of **2** may lead to conformations of four chelating arms of cyclam moieties in such a way that the complexation of the Eu^{III} may not always be possible.

Thus, Eu^{III} ions are probably eight-coordinate in the same way as Eu^{III} within **S4a** (Figure 5), but also in a different way as proposed in Figure 6 (coordination with the four nitrogen atoms of the macrocycle and four oxygen atoms of amido groups originating from different macrocycles) which could explain the luminescence data for $\text{S2}[\text{Eu}(\text{NO}_3)_3]$.

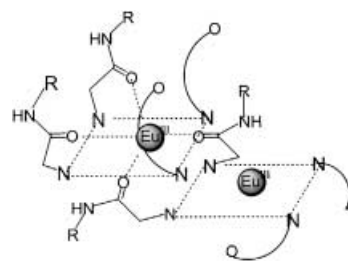


Figure 6. Proposed coordination mode within $\text{S2}[\text{Eu}(\text{NO}_3)_3]$.

*Coordination mode of Eu^{III} within **S1**:* The thermal analyses of $\text{S1}[\text{Eu}(\text{NO}_3)_3]$ have shown that the nitrate groups are not bidentate to Eu^{III} .

The luminescence properties of $\text{S1}[\text{Eu}(\text{NO}_3)_3]$ suggest the presence of several Eu^{III} bonding sites within the xerogels.

We propose a coordination mode of one Eu^{III} /two cyclam moieties, in agreement with the elemental analysis data of the xerogel $\text{S1}[\text{Eu}(\text{NO}_3)_3]$ and of co-gels $\text{S}_y\mathbf{1}[\text{Eu}(\text{NO}_3)_3]$. This result involves the location of cyclam moieties in close proximity to each other. The same conclusion was reached in a study of the incorporation of Cu^{II} in this same material.^[7] Eu^{III} would be eight-coordinate and located between two planes, each defined by four nitrogen atoms. Such complexation is unlikely in solution. Indeed, whereas a number of examples of lanthanide complexes resulting from coordination $4\text{N}+4\text{O}$ have been reported,^[24–26] to the best of our knowledge there is no example of $4\text{N}+4\text{N}$ coordination of lanthanide ions. The four nitrogen atoms could originate from the same macrocycle or from different rings (Figure 7), which would explain the luminescence behaviour of these materials. It is important that, in this case, the incorporation of Eu^{III} is controlled by the self-assembly of the cyclam moieties during the sol–gel process on one hand, and by the weak entropy of the system on the other.

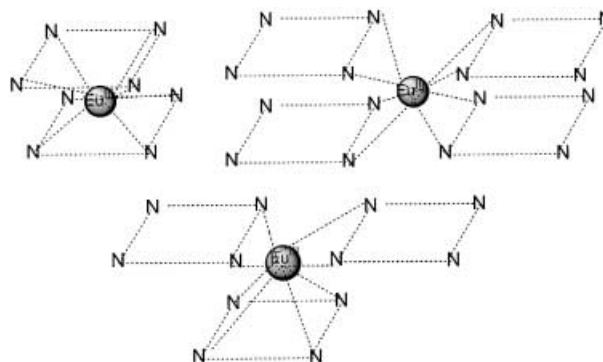


Figure 7. Possible modes of $4\text{N}+4\text{N}$ coordination within $\text{S1}[\text{Eu}(\text{NO}_3)_3]$.

*Coordination mode of Eu^{III} within **S3**:* The FTIR spectrum of $\text{S3}[\text{Eu}(\text{NO}_3)_3]$ indicated that all the $\text{C}=\text{O}$ groups are not coordinated to Eu^{III} . The thermal analysis of this same xerogel revealed that the nitrate groups are probably bidentate to the Eu^{III} . The Eu^{III} uptake is more than one Eu^{III} /cyclam moiety.

In this case, each N-substituted cyclam unit is unable to complex a Eu^{III} in solution because the amido groups are not in an appropriate geometry. However, in the solid the

situation is very different. Each cyclam unit introduces into the solid four nitrogen and four amido groups, the distribution of which is dependent on the conformations resulting from the sol–gel process. Thus, that the Eu^{III}/cyclam moiety ratio exceeds unity can be explained by taking into account the behaviour of the nitrate groups as bidentate ligands, in addition to the other chelating groups (tetraazamacrocycles and amido groups). This would give rise to several types of coordination, in agreement with the luminescence spectrum of **S3**[Eu(NO₃)₃].

Conclusion

We have shown that the coordination mode of europium salts within solids is not the same as in solution. In particular we have found that Eu^{III} uptake into hybrid material incorporating cyclam moieties containing *N*-alkyl substituents is possible, because during the sol–gel process cyclam moieties are arranged so that they are in close proximity to each other. Their proximity gives rise to Eu^{III} complexes of type 4N+4N in the case of the incorporation of Eu^{III} into the material **S1**, whereas Cu^I incorporation into the same material leads to the formation of copper–copper interactions.^[7]

Experimental Section

General: All air-sensitive manipulations were carried out in a dry argon atmosphere using standard Schlenk techniques. All solvents were dried carefully and distilled before use. The ¹H and ¹³C NMR solution spectra were recorded on a Bruker DPX200 (at 200 MHz for ¹H and 50 MHz for ¹³C), and the ²⁹Si NMR spectra on a Bruker AC200 (at 40 MHz). Chemical shifts are reported as δ values. They are referenced to Me₄Si (¹H, ¹³C, ²⁹Si). Multiplicity is indicated as follows: s, singlet; d, doublet; t, triplet; q, quartet; m, multiplet.

Cross-polarisation magic-angle spinning (CP MAS) ²⁹Si as well as CP MAS ¹³C NMR spectra were recorded on a Bruker FTAM300 (repetition times 5 and 10 s with contact times of 5 and 2 ms). IR spectra were recorded on a Perkin-Elmer 1600 spectrometer. Fast atom bombardment (FAB) mass measurements [matrix, *m*-nitrobenzyl alcohol (NBA)] were registered on a JEOL JMS-D3000 spectrometer. Specific surface areas were determined by the Brunauer–Emmett–Teller (BET) method on Micromeritics ASAP2010 and Micromeritics Gemini III2375 analysers. Melting points were measured with a Büchi B-540. Microanalyses were performed by the Service Central d'Analyse (CNRS, France). Bromoacetyl bromide, *p*-(chloromethyl)benzoyl chloride, tetraethoxysilane (TEOS), Eu(NO₃)₃·6H₂O and EuCl₃·6H₂O were purchased from Acros. Aminopropyltriethoxysilane was supplied by Aldrich. Photoluminescence measurements were performed at low temperature (2 K) using the 325 nm radiation of a He–Cd laser as the excitation source, operating at 10 mW power. Sample cooling was provided by a closed-cycle He optical cryostat (Cryomech GB-15). Excitation spectra were recorded using a Xe lamp.

2-Bromo-*N*-triethoxysilylpropylacetamide: A solution of bromoacetyl bromide (21.7 g, 107.4 mmol) in anhydrous diethyl ether (150 mL) was added dropwise at –80 °C under stirring to a mixture of freshly distilled triethylamine (10.85 g, 107.4 mmol) and of aminopropyltriethoxysilane (22.6 g, 102.3 mmol) in anhydrous ether (350 mL). When the addition was complete, the mixture was allowed to warm to 20 °C. The ammonium salts were filtered and washed with anhydrous diethyl ether under argon. The filtrate was then concentrated. A red oil was obtained and distilled under vacuum to give a colourless oil (22.8 g, 66.7 mmol, 65%). B.p._{0.05 mmHg} 135–140 °C; ¹H NMR (200 MHz, CDCl₃): δ = 0.59 (m, 2H), 1.17 (t, ³J = 7.0 Hz, 9H), 1.62 (m, 2H), 3.25 (m, 2H), 3.78 (q, ³J = 7.0 Hz, 6H), 3.83 (s, 2H), 6.88 ppm (m, 1H); ¹³C NMR (50 MHz, CDCl₃): δ = 7.74, 18.38, 22.76, 29.23,

42.56, 58.57, 165.73 ppm; ²⁹Si NMR (40 MHz, CDCl₃): δ = –45.71 ppm (s); IR (NaCl): $\tilde{\nu}$ = 3291.0, 3084.6, 1653.8 cm^{–1}.

***p*-Chloromethyl-*N*-triethoxysilylpropylbenzamide:** A solution of *p*-(chloromethyl)benzoyl chloride (4.8 g, 26.4 mmol) in anhydrous diethyl ether (40 mL) was added dropwise at –80 °C under stirring to a mixture of freshly distilled triethylamine (2.7 g, 26.9 mmol) and of aminopropyltriethoxysilane (5.8 g, 26.4 mmol) in anhydrous diethyl ether (100 mL). After exactly the same procedure as for 2-bromo-*N*-triethoxysilylpropylacetamide, a colorless oil (6.3 g, 16.8 mmol, 66%) was obtained. B.p._{0.04 mmHg} 145–150 °C; ¹H NMR (200 MHz, CDCl₃): δ = 0.70 (m, 2H), 1.22 (t, ³J = 7.0 Hz, 9H), 1.75 (m, 2H), 3.46 (m, 2H), 3.82 (q, ³J = 7.0 Hz, 6H), 4.60 (s, 2H), 6.63 (m, 1H), 7.37 (d, ³J = 8.5 Hz), 7.77 ppm (d, ³J = 8.5 Hz, 2H); ¹³C NMR (50 MHz, CDCl₃): δ = 8.07, 18.52, 23.08, 42.47, 45.67, 58.75, 127.59, 128.85, 135.15, 140.78, 167.12 ppm; ²⁹Si NMR (40 MHz, CDCl₃): δ = –45.30 ppm (s); IR (NaCl): $\tilde{\nu}$ = 3316.2, 3070.5, 1637.8 cm^{–1}.

1,4,8,11-Tetrakis[3-(triethoxysilylpropylcarbamoyle)methyl]-1,4,8,11-tetraazacyclotetradecane (2): A solution of 2-bromo-*N*-triethoxysilylpropylacetamide (11.1 g, 32.5 mmol) in anhydrous acetonitrile (25 mL) was added dropwise at 20 °C to a suspension of 1,4,8,11-tetraazacyclotetradecane (cyclam) (1.6 g, 8.05 mmol) and of potassium carbonate in anhydrous acetonitrile (80 mL). The reaction mixture was heated under reflux for 12 h. The solvent was removed under vacuum. The white residue was taken up again in CH₂Cl₂. After filtration of salts, the filtrate was concentrated to give a white solid (9.7 g, 7.77 mmol, 97%). M.p. 108.7–110.4 °C; ¹H NMR (200 MHz, CDCl₃): δ = 0.59 (m, 8H), 1.20 (t, ³J = 7.0 Hz, 36H), 1.58 (m, 12H), 2.58–2.62 (m, 16H), 3.02 (s, 8H), 3.22 (m, 8H), 3.79 (q, ³J = 7.0 Hz, 24H), 7.03 ppm (t, ³J = 5.7 Hz, 4H); ¹³C NMR (50 MHz, CDCl₃): δ = 8.15, 18.52, 23.64, 24.67, 41.89, 51.16, 52.38, 58.61, 58.89, 170.67 ppm; ²⁹Si NMR (40 MHz, CDCl₃): δ = –45.77 ppm (s); IR (NaCl): $\tilde{\nu}$ = 3273.5, 3070.5, 1684.0, 1646.1 cm^{–1}; C₅₄H₁₁₆O₁₆N₈Si₄; calcd: C 52.06, H 9.38, Si 9.02, N 8.99; found: C 51.82, H 9.12, Si 9.20, N 8.93.

1,4,8,11-Tetrakis(*p*-methyl-*N*-triethoxysilylpropylbenzamide)-1,4,8,11-tetraazacyclotetradecane (3): This was prepared by the same procedure as **2**. The starting reagents were the cyclam (0.83 g, 4.15 mmol), potassium carbonate (5.1 g, 37.2 mmol) in anhydrous acetonitrile (65 mL) and *p*-chloromethyl-*N*-triethoxysilylpropylbenzamide (6.3 g, 16.7 mmol) in anhydrous acetonitrile (15 mL). Compound **3** was obtained as a slightly yellow powder (4.9 g, 3.15 mmol, 76%). M.p. 139.8–140.9 °C; ¹H NMR (200 MHz, CDCl₃): δ = 0.71 (m, 8H), 1.21 (t, ³J = 7.0 Hz, 36H), 1.76 (m, 12H), 2.37–2.53 (m, 16H), 3.42–3.50 (m, 16H), 3.81 (q, ³J = 7.0 Hz, 24H), 6.80 (t, ³J = 5.8 Hz, 4H), 7.27 (d, ³J_{H,H} = 8.2 Hz, 8H), 7.65 ppm (d, ³J_{H,H} = 8.2 Hz, 8H); ¹³C NMR (50 MHz, CDCl₃): δ = 8.01, 18.42, 23.07, 24.34, 42.50, 50.93, 51.88, 58.58, 59.31, 126.94, 128.95, 133.50, 143.66, 167.65 ppm; ²⁹Si NMR (40 MHz, CDCl₃): δ = –45.22 ppm (s); IR (NaCl): $\tilde{\nu}$ = 3226.9, 1637.8 cm^{–1}; C₇₈H₁₃₂O₁₆N₈Si₄; calcd: C 60.43, H 8.58, Si 7.25, N 7.23; found: C 59.92, H 8.57, Si 7.00, N 7.68.

Complex 4a: A solution (0.2 M) of **2** (1.5 g, 1.21 mmol) in boiling anhydrous ethanol (25 mL) was added to a boiling ethanol solution containing anhydrous europium nitrate^[27] (1 equiv, 50 mmol L^{–1}). The reaction mixture was heated under reflux for 2 h, then left to stand at room temperature for 12 h. The precipitate was filtered; the filtrate was concentrated and the solid was washed with pentane and dried under vacuum. The product was obtained as a white solid (1.7 g, 1.09 mmol, 90%). M.p. 82.1–82.9 °C; ¹H NMR (200 MHz, CDCl₃): δ = 0.60 (m, 8H), 1.21 (t, ³J = 7.0 Hz, 36H), 1.56–1.62 (m, 12H), 1.76 (m, 12H), 2.61–2.65 (m, 16H), 3.03 (s, 8H), 3.21 (m, 8H), 3.80 (q, ³J = 7.0 Hz, 24H), 7.27 ppm (t, ³J = 5.7 Hz, 4H); ¹³C NMR (50 MHz, CDCl₃): δ = 8.26, 18.66, 23.77, 24.75, 42.03, 51.24, 52.48, 58.76, 60.00, 170.84 ppm; ²⁹Si NMR (40 MHz, CDCl₃): δ = –45.78 ppm (s); IR (NaCl): $\tilde{\nu}$ = 3284.2, 3081.2, 1648.5, 1621.8 cm^{–1}; MS (FAB⁺, NBA): *m/z* (%): 1395 (100) [(M+H) – 3NO₃]⁺.

Complex 4b: This was prepared by the same procedure as **4a**, from **2** (3.0 g, 2.41 mmol) in anhydrous ethanol (40 mL). The product was obtained as a white solid (3.3 g, 2.21 mmol, 91%). M.p. 72.1–73.5 °C; IR (NaCl): $\tilde{\nu}$ = 3220.1, 3049.1, 1648.5, 1621.8 cm^{–1}; MS (FAB⁺, NBA): *m/z* (%): 1395 (100) [(M+H) – 3Cl]⁺; C₅₄H₁₁₆O₁₆Cl₃EuN₈Si₄; calcd: C 43.11, H 7.77, Si 7.47, N 7.45, Eu 10.10; found: C 41.99, H 7.48, Si 7.50, N 7.28, Eu 10.65.

Preparation of xerogels: The hydrolysis and polycondensation of the europium complexes was carried out by the procedure exemplified by the preparation of **S4a**.

Xerogel S4a: A solution of **4a** (1.50 g, 0.95 mmol) in THF (1.19 mL) was placed in a 35 mL Pyrex test tube. A sample (1.19 mL) of a THF solution (6 M in H₂O (5.69 mmol) and 0.1 M in HCl (10% mol)) was added dropwise at room temperature with a syringe. After it had been stirred for 3 min, the solution was placed in a thermostatted water-bath at 30 °C without stirring. A translucent gel was formed after 4 h 30 min. The wet translucent gel was allowed to age for five days at 30 °C, after which it was powdered and washed with acetonitrile and ether. The gel was powdered again and dried under vacuum (0.1 mmHg) for 13 h at 120 °C yielding 0.99 g of a white powder. $S_{\text{BET}} < 10 \text{ m}^2 \text{ g}^{-1}$; IR (DRIFT, KBr): $\tilde{\nu} = 3504, 1649, 1622 \text{ cm}^{-1}$; C₃₀EuH₅₆N₁₁O₁₉Si₄: calcd: C 31.63, H 4.96, N 13.53, Si 9.86; found: C 33.47, Eu 11.40, H 6.00, N 11.81, Si 9.50.

S4b: $S_{\text{BET}} < 10 \text{ m}^2 \text{ g}^{-1}$; IR (DRIFT, KBr): $\tilde{\nu} = 3504, 1649, 1622 \text{ cm}^{-1}$; C₃₀Cl₃EuH₅₆N₈O₁₀Si₄: calcd: C 34.00, Cl 10.05, Eu 14.34, H 5.33, N 10.58, Si 10.60; found: C 34.31, Cl 8.75, Eu 13.75, H 6.39, N 8.71, Si 8.85.

The hydrolysis and polycondensation of precursors **1–3** were carried out by the procedure exemplified by the preparation of **S1**: a 2.45 mL sample of a THF solution containing H₂O (0.21 mL, 11.8 mmol) and 1 M in THF (1 mol%) was added dropwise at room temperature to a solution of **1** (2.00 g, 1.97 mmol) in THF (2.46 mL). After 3 min stirring, the solution was placed in a thermostatted water-bath at 30 °C without stirring. A translucent gel was formed after 2 h 30 min. After five days aging at 30 °C, the gel was powdered and washed with acetonitrile and diethyl ether. It was powdered again and dried under vacuum (0.1 mmHg) for 13 h at 120 °C yielding 1.19 g of a white powder. $S_{\text{BET}} = 315 \text{ m}^2 \text{ g}^{-1}$; TGA (weight loss [T]): 0.9% [25–150 °C]; 18.2% [220–400 °C]; 39.5% [400–1100 °C]; ¹³C NMR (75 MHz, CP MAS): $\delta = 12.5, 24.77, 24.0, 30.0, 54.7, 57.8$; ²⁹Si NMR (60 MHz, CP MAS): $\delta = -45.2 \text{ (T}^1\text{)}, -59.1 \text{ (T}^2\text{)}, -66.3 \text{ (T}^3\text{)}$; C₂₂H₄₄N₄O₆Si₄: calcd: C 46.12, H 7.74, N 9.78, Si 19.61; found: C 43.60, H 7.59, N 8.35, Si 17.45.

Xerogel S2: $S_{\text{BET}} < 10 \text{ m}^2 \text{ g}^{-1}$; TGA (weight loss [T]): 3.0% [25–120 °C], 36.9% [200–550 °C]; 27.6% [550–1200 °C]; ²⁹Si NMR (60 MHz, CP MAS): $\delta = -57.9 \text{ (T}^1\text{)}, -65.0 \text{ (T}^2\text{)}, -77.0 \text{ (T}^3\text{)}$; C₃₀H₅₆N₈O₁₀Si₄: calcd: C 44.97, H 7.05, N 13.99, Si 14.02; found: C 43.16, H 7.19, N 12.87, Si 13.37.

Xerogel S3: $S_{\text{BET}} < 10 \text{ m}^2 \text{ g}^{-1}$; TGA (weight loss [T]): 0.9% [25–150 °C]; 33.9% [200–500 °C], 32.7% [500–1220 °C]; ¹³C NMR (75 MHz, CP MAS): $\delta = 10.4, 23.8, 43.2, 58.5, 128.9, 144.4, 168.9$; ²⁹Si NMR (60 MHz, CP MAS): $\delta = -57.4 \text{ (T}^2\text{)}, -65.9 \text{ (T}^3\text{)}$; C₃₄H₇₂N₈O₁₀Si₄: calcd: C 58.67, H 6.56, N 10.14, Si 10.16; found: C 57.54, H 6.67, N 9.55, Si 7.80.

Direct incorporation of Eu(NO₃)₃·6H₂O and of EuCl₃·6H₂O into the xerogels SZ (Z = 1–3) (route B): Europium salts were incorporated into xerogels **SZ** (Z = 1–3) by the same procedure in all cases. Just before reaction, the xerogels were dried for 14 h at 120 °C under vacuum (0.1 mmHg). The incorporation of Eu(NO₃)₃·6H₂O into **S1** is given as an example.

Incorporation of Eu(NO₃)₃·6H₂O into S1: Xerogel **S1** (600 mg, 1.05 mmol) and Eu(NO₃)₃·6H₂O (0.93 g, 2.09 mmol) in absolute alcohol (35 mL) were placed in a Pyrex tube (35 mL). After it had been stirred for 14 h under reflux (78 °C), the suspension was filtered, then washed with ethanol until there was no trace of europium nitrate in the filtrates. After 13 h of drying under vacuum (0.1 mmHg) at 120 °C, a white powder (532 mg) was obtained. $S_{\text{BET}} < 10 \text{ m}^2 \text{ g}^{-1}$; TGA (weight loss [T]): 1.9% [25–130 °C]; 41.5% [215–225 °C], 8.4% [225–335 °C], 16.2% [335–695 °C], 2.9%

[695–1080 °C]; C₂₂H₄₄Eu_{0.51}N_{5.5}O_{10.5}Si₄: calcd: C 35.61, H 5.98, Eu 10.24, N 10.38, Si 15.14; found: C 31.62, H 6.08, Eu 8.60, N 8.81, Si 12.45 (that is, C_{23.8}H_{54.4}Eu_{0.51}N_{5.7}Si_{4.0}).

Incorporation of EuCl₃·6H₂O into S1: $S_{\text{BET}} < 10 \text{ m}^2 \text{ g}^{-1}$; TGA (weight loss [T]): 20.1% [200–350 °C], 34.6 [350–950 °C], 2.0% [900–1250 °C]; C₂₂H₄₄Cl_{1.5}Eu_{0.5}N₄O₆Si₄: calcd: C 37.63, H 6.32, Cl 7.58, Eu 10.82, N 7.98, Si 16.00; found: C 31.53, H 6.64, Cl 10.77, Eu 11.90, N 6.43, Si 13.40 (that is, C_{22.0}H_{55.2}Cl_{2.54}Eu_{0.65}N_{3.9}Si_{4.0}).

Incorporation of Eu(NO₃)₃·6H₂O into S2: $S_{\text{BET}} < 10 \text{ m}^2 \text{ g}^{-1}$; TGA (weight loss [T]): 1.5% [25–130 °C]; 31.3% [258–268 °C], 33.3% [268–1200 °C]; IR (DRIFT, KBr): $\tilde{\nu} = 3092, 1648, 1624, 1547, 1456, 1317 \text{ cm}^{-1}$; C₃₀H₅₆EuN₁₁O₁₉Si₄: calcd: C 31.63, H 4.96, Eu 13.34, N 13.53, Si 9.86; found: C 31.24, H 5.53, Eu 12.10, N 11.51, Si 10.50 (that is, C_{35.1}H_{58.7}Eu_{0.85}N_{8.8}Si_{4.0}).

Incorporation of EuCl₃·6H₂O into S2: $S_{\text{BET}} < 10 \text{ m}^2 \text{ g}^{-1}$; TGA (weight loss [T]): 23.6% [200–400 °C], 10.7% [400–550 °C], 27.9% [550–1250 °C]; IR (DRIFT, KBr): $\tilde{\nu} = 3071, 1653, 1627, 1542 \text{ cm}^{-1}$; C₃₀H₅₆Cl₃EuN₈O₁₀Si₄: calcd: C 34.00, H 5.33, Cl 10.05, Eu 14.34, N 10.58, Si 10.60; found: C 34.94, H 6.51, Cl 7.76, Eu 10.95, N 10.19, Si 10.25 (that is, C_{29.8}H_{66.8}Cl_{2.24}Eu_{0.74}N_{7.5}Si_{4.0}).

Incorporation of Eu(NO₃)₃·6H₂O into S3: $S_{\text{BET}} < 10 \text{ m}^2 \text{ g}^{-1}$; TGA (weight loss [T]): 16.6% [205–345 °C]; 15.9% [345–505 °C], 36.6% [505–1065 °C]; IR (DRIFT, KBr): $\tilde{\nu} = 3060, 1644, 1627, 1547, 1456, 1307 \text{ cm}^{-1}$; C₃₄H₇₂EuN₁₁O₁₉Si₄: calcd: C 44.93, H 5.03, Eu 10.53, N 10.67, Si 7.78; found: C 42.73, H 5.36, Eu 11.00, N 9.95, Si 7.25 (that is, C_{53.9}H_{82.4}Eu_{1.12}N_{11.0}Si_{4.0}).

Preparation of co-gels S_y1 and S_y2 (y = 5, 10, 15, 40): All the co-gels were prepared by the procedure exemplified by the preparation of **S₅1**: **1** (1.50 g, 1.48 mmol) and TEOS (1.45 g, 7.38 mmol) were placed in a Schlenk in THF (6.6 mL). A 6.6 mL sample of a THF solution containing H₂O (0.43 mL, 23.62 mmol) and 1 M in TBAF (1 mol%) was added dropwise at 20 °C to a solution of **3** (1.50 g, 1.48 mmol) and of TEOS (1.45 g, 7.38 mmol) in THF (6.6 mL). After 3 min of stirring, the solution was placed in a thermostatted water-bath at 30 °C without stirring. A gel was formed after 50 min. The wet gel was allowed to age for five days at 30 °C, after which it was powdered and washed with ethanol, acetone and diethyl ether. After drying for 13 h under vacuum (0.1 mmHg) at 120 °C, 1.37 g of a white powder was obtained.

The textural characteristics of **S_y1** and **S_y2** are given in Table 6.

Incorporation of Eu(NO₃)₃·6H₂O into the co-gels S_y1 and S_y2 (y = 5, 10, 15, 40): The co-gels were treated with Eu(NO₃)₃·6H₂O as indicated in the Results and Discussion section. The textural characteristics of the resulting solids are given in Table 7.

Table 6. Some relevant physicochemical characteristics of co-gels **S_y1** and **S_y2**.

	S₅1	S₁₀1	S₁₅1	S₄₀1	S₅2	S₁₀2	S₁₅2	S₄₀2
$S_{\text{BET}} [\text{m}^2 \text{ g}^{-1}]$	650	760	750	640	60	380	480	500
pore volume [$\text{cm}^3 \text{ g}^{-1}$]	0.48	0.89	1.09	0.70	–	0.63	0.81	0.36
Dp [Å]	30–40	30–70	50–90	50–90	–	50–200	80–400	> 500

Table 7. Some relevant physicochemical characteristics of co-gels **S_y1[Eu(NO₃)₃]** and **S_y2[Eu(NO₃)₃]**.

	S₅1[Eu(NO₃)₃]	S₁₀1[Eu(NO₃)₃]	S₁₅1[Eu(NO₃)₃]	S₅2[Eu(NO₃)₃]	S₁₀2[Eu(NO₃)₃]	S₁₅2[Eu(NO₃)₃]
$S_{\text{BET}} [\text{m}^2 \text{ g}^{-1}]$	480	610	640	20	250	340
pore volume [$\text{cm}^3 \text{ g}^{-1}$]	0.35	0.72	0.96	–	0.52	0.98
Dp [Å]	30–40	30–70	50–90	30–40	30–70	50–90

- [6] B. Boury, F. Ben, R. Corriu, *Angew. Chem. Int. Ed.* **2001**, *40*, 2853.
- [7] G. Dubois, C. Rey , R. J. P. Corriu, S. Brand s, F. Denat, R. Guillard, *Angew. Chem.* **2001**, *113*, 1121; *Angew. Chem. Int. Ed.* **2001**, *40*, 1087.
- [8] M. Lachkar, R. Guillard, A. Atmani, A. De Cian, J. Fisher, R. Weiss, *Inorg. Chem.* **1998**, *37*, 1575.
- [9] R. Corriu, C. Rey , A. Mehdi, G. Dubois, C. Chuit, F. Denat, B. Roux-Fouillet, R. Guillard, G. Lagrange, S. Brand s, FR 2774093, July 30, **1999**.
- [10] F. S. Richardson, *Chem. Rev.* **1982**, *82*, 541.
- [11] J-C. Bunslı, G. R. Choppin, *Lanthanide Probes in Life, Chemical, and Earth Sciences*, Elsevier, New York, **1989**.
- [12] R. Guillard, B. Roux-Fouillet, G. Lagrange, M. Meyer, A. Bucaille, WO O14602, June 28, **2001**.
- [13] G. Dubois, C. Rey , R. J. P. Corriu, S. Brand s, F. Denat, R. Guillard, *Chem. Commun.* **1999**, 2283.
- [14] O. A. Ganson, A. R. Kausar, M. J. Weaver, E. L. Lee, *J. Am. Chem. Soc.* **1977**, *99*, 7087.
- [15] E. Lee, O. A. Ganson, M. J. Weaver, *J. Am. Chem. Soc.* **1980**, *102*, 2278.
- [16] M. Magi, E. Lippmaa, A. Samoson, G. Engelhardt, A. R. Grimmer, *J. Phys. Chem.* **1984**, *88*, 1518.
- [17]
$$\tau = \frac{0.5 \times (\text{area T}^1) + 1.0 \times (\text{area T}^2) + 1.5 \times (\text{area T}^3)}{1.5}$$
- [18] K. J. Shea, D. A. Loy, O. Webster, *J. Am. Chem. Soc.* **1992**, *114*, 6700.
- [19] G. Cerveau, R. J. P. Corriu, C. Lepeytre, P. H. Mutin, *J. Mater. Chem.* **1998**, *8*, 2707.
- [20] B. Ribar, A. Kapor, G. Argay, A. Kalman, *Acta Crystallogr., Sect. C* **1983**, 39.
- [21] R. D. Hancock, A. E. Martell, *Chem. Rev.* **1989**, *89*, 1875.
- [22] R. D. Hancock, H. Maumela, A. S. Desousa, *Coord. Chem. Rev.* **1996**, *148*, 315.
- [23] M. Meyer, V. Dahaoui-Gindrey, C. Lecomte, R. Guillard, *Coord. Chem. Rev.* **1998**, *178–180*, 1313.
- [24] J. R. Morrow, S. Amin, C. H. Lake, M. R. Churchill, *Inorg. Chem.* **1993**, *32*, 4566.
- [25] S. Amin, J. R. Morrow, C. H. Lake, M. R. Churchill, *Angew. Chem.* **1994**, *106*, 824; *Angew. Chem. Int. Ed. Engl.* **1994**, *33*, 773.
- [26] R. S. Dickins, J. A. K. Howard, C. W. Lehmann, J. Moloney, D. Parker, R. D. Peacock, *Angew. Chem.* **1997**, *109*, 541; *Angew. Chem. Int. Ed. Engl.* **1997**, *36*, 521.
- [27] F. Embert, A. Medhi, C. Rey , R. J. P. Corriu, *Chem. Mater.* **2001**, *13*, 4542.

Received: November 8, 2001
Revised: June 27, 2002 [F3668]